Đorđe Đurđević[1], Simon Sedmak[2], Andrijana Đurđević[1], Nina Anđelić[3], Taško Maneski[3]

DEVELOPMENT AND CALCULATION OF SUPPORTING STRUCTURE FOR MINING POWER EQUIPMENT

RAZVOJ I PRORAČUN NOSEĆE KONSTRUKCIJE RUDARSKE ELEKTROENERGETSKE OPREME

Originalni naučni rad / Original scientific paper
UDK /UDC:

Rad primljen / Paper received: 28.6.2021

Adresa autora / Author's address:
[1)] Tehnikum Taurunum - College of Applied Engineering Studies, Belgrade, Serbia,
email: djdjurdjevic@tehnikum.edu.rs
[2)] University of Belgrade, Innovation Centre of the Faculty of Mechanical Engineering, Belgrade, Serbia
[3)] University of Belgrade, Faculty of Mechanical Engineering, Belgrade, Serbia

Keywords
- mining equipment
- supporting structure
- equivalent stress
- finite element method (FEM)
- deformation

Ključne reči
- rudarska oprema
- noseća konstrukcija
- ekvivalentni napon
- metoda konačnih elemenata (FEM)
- deformacija

Abstract

Development and calculation of the base supporting structure used for mining equipment is the aim of the paper. The base structure is intended for the installation of electronic communication and power equipment and devices that supply and manage mining equipment. The first part of the paper covers the existing solutions, and the second part shows the development of a new solution. Design solution of a new base structure is presented, a calculation of the base according to valid standards and regulations, and the numerical determination of equivalent stress and strain by Abaqus® software. Finally, the performed solution is given.

Izvod

Cilj ovog rada jeste razvoj i proračun postolja noseće konstrukcije, koja se koristi za rudarsku opremu. Postolje je namenjeno za smeštaj elektronsko komunikacione i elektroenergetske opreme i uređaja koji napajaju i upravljaju rudarskom opremom. U prvom delu rada, prikazana su postojeća rešenja, a u drugom delu je prikazan razvoj novog rešenja. U radu je predstavljen, pored projektovanja novog rešenja, proračun prema važećim standardima i propisima i numeričko određivanje ekvivalentnog napona i deformacije u softveru Abaqus®. Na kraju rada je predstavljeno izvedeno rešenje.

INTRODUCTION

The paper presents the numerical analysis of stress distribution in a supporting structure mainly used in mining applications, /1-6/, along with fracture mechanics principles, which are applied to one of the connection lugs, in order to determine structural behaviour in the presence of a crack.

The support system presented here is developed in cooperation with companies Eurometal (Ub, Serbia) and Schneider Electric. The system is used for installing electronic communication and power generation devices for various types of mining equipment. Its main purpose is to provide stability and safe transportation of the contained equipment, which includes the possibility of being lifted by cranes or forklifts during exploitation in mines.

The supplier of electronic equipment for communication and power generation, Scheider Electric, also defined the input parameters and conditions that this equipment must fulfil in order to function in a reliable and safe manner. This included working conditions, safety, transport, storage, and installation of the support system.

EXISTING AND NEW SOLUTION

Figure 1 shows the current solution for the support system, along with rear cable holes which allow cables to be connected to the equipment, from ground level, through the metal supports. Figure 1a shows the version with three cells, whereas Fig. 1b shows the two cell support system. The new suggested solution is shown in Fig. 2, including various cross-sections and a detailed schematic view of all supporting elements.

In the following, the analytically obtained results for stress distribution in a biaxially loaded isotropic plate with a rectangular opening are shown, /7, 8/. The isotropic plate, shown in Fig. 1, is of finite dimensions and has a rectangular opening at its centre, with a side ratio $a/b = 3/2$, and a fillet radius of $r = (3/50)a$, where the opening side a is parallel to the x axis, and side b is parallel to the y axis. The plate is subjected to tension in two mutually perpendicular directions via surface forces with intensity q along the x direction and p along the y direction.

During the mapping of the observed area with a rectangular opening to the interior of a unit circle with radius $r = 1$, according to the procedure given in /7, 8/, the expres-

sions for stress components in polar coordinates have the following form:

$$\sigma_r = \frac{1}{r}\frac{\partial \Phi}{\partial r} + \frac{1}{r^2}\frac{\partial^2 \Phi}{\partial \theta^2},\ \sigma_\theta = \frac{\partial^2 \Phi}{\partial r^2},\ \tau_{r\theta} = -\frac{\partial}{\partial r}\left(\frac{1}{r}\frac{\partial \Phi}{\partial \theta}\right).$$

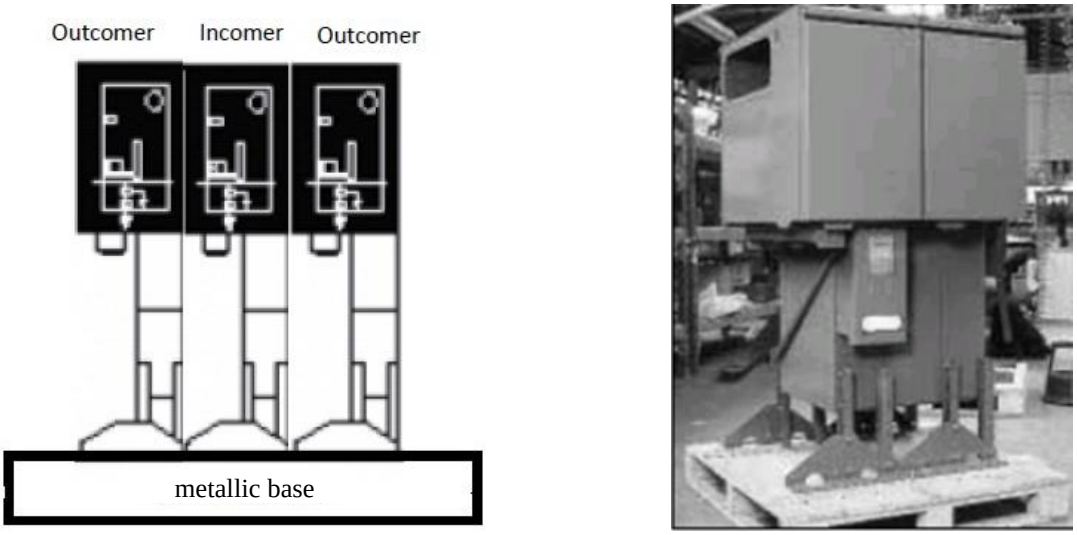

a) three cells b) two cells

Figure 1. The current solution.

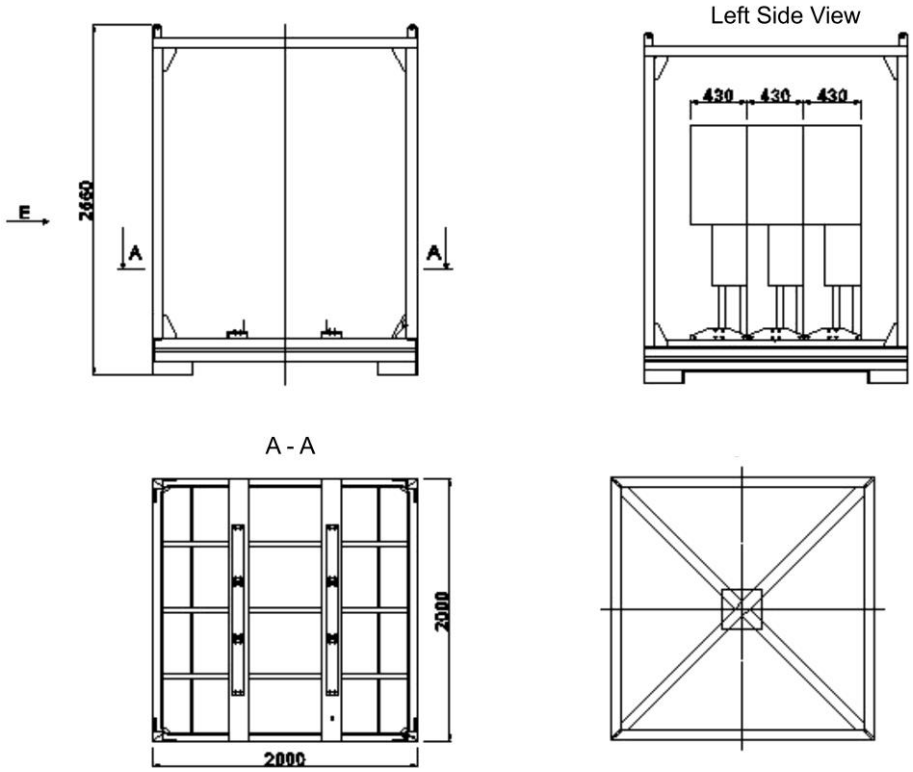

Figure 2. The new solution for the supporting system design.

As can be seen from the above figure, the supporting system is an assembly made of steel elements (standard sheets and profiles), whose centre mass is located in its upper zone. For the sake of stability and based on standard calculations, it is decided to add concrete to the base of the supporting system, in order to move the centre mass closer to the base, /1-8/. The equipment is connected to the supporting structure via M16 and M10 screws. The base of the supporting system is to be made of standard rectangular, box and bent steel profiles and sheets.

Dimensions of the supporting system are - length and width of 2 m, and height of 2.66 m. Its weight is 2338 kg, whereas the equipment to be installed weighs 900 kg.

The floor base is made of hot-rolled standard profiles UNP180 and INP80, bent according to the relevant documentation (S235JR-EN10025). DC01-EN10130 sheets with a thickness of 2 mm are placed on the top and bottom side of the floor, and continually welded to the base structure. In addition, transversal supports are placed in the bottom zone of the floor, including INP80 profiles.

The top side of the floor also incorporates INP80 profiles, along with longitudinal supports of dimensions 150×5×4 (bent), used for connecting the equipment. The connection between the top and bottom profiles is achieved by welding them to UNP300 profiles.

The supporting frame is made by welding, and the bars are welded to the supporting base. These elements are made using box profiles (80×80×4).

Constant load in a structure refers to all loads that do not change over a short time period, and in this case it includes the weight of the steel structure, weight of concrete, and the weight of the equipment.

NUMERICAL SIMULATIONS

Numerical calculations are performed using finite element method, /9-12/. Mechanical properties of steel S235JRG2 are shown in Table 1, /13/. ABAQUS® software is used for this simulation with units [m], [N], and [kg]. Figures 3-7 show numerical models with boundary conditions and loads, equivalent stresses and their normal and shear components, and displacements, respectively.

Table 1. Mechanical properties of steel S235JRG2.

Young's modulus [Pa]	Poisson's ratio	Yield stress [Pa]	Allowable stress [Pa]
$2.1 \cdot 10^{11}$	0.3	$235 \cdot 10^{6}$	$160 \cdot 10^{6}$

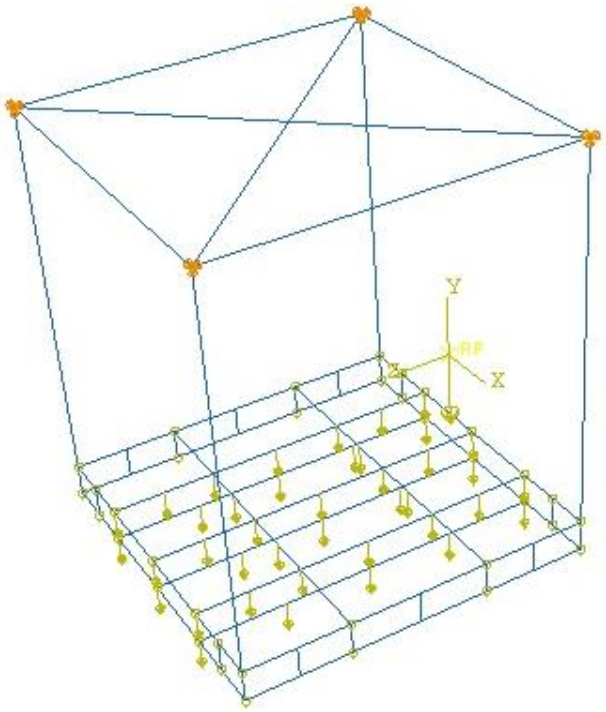

Figure 3. Loads and boundary conditions.

Figure 4 shows the distribution of equivalent stress to Hencky-Mises hypothesis in [Pa], and as it can be seen the values are well below allowed stress levels for this material. It can be concluded from the results shown in Figs. 5 and 6 that the normal stresses are the dominant component, being almost equal to the equivalent stress value. Maximum displacement in the model is around 8.1 mm, which is well within the allowed limits.

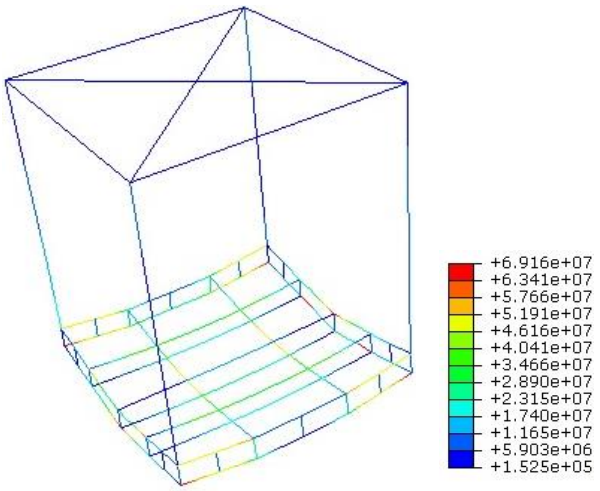

Figure 4. Equivalent stress according to Hencky-Mises in [Pa].

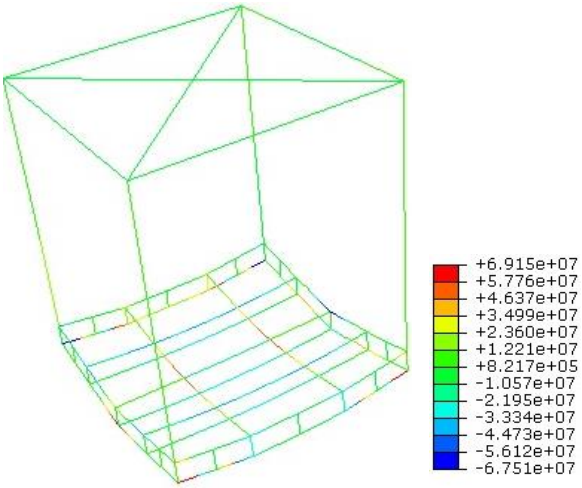

Figure 5. Normal stresses σ_{12} in [Pa].

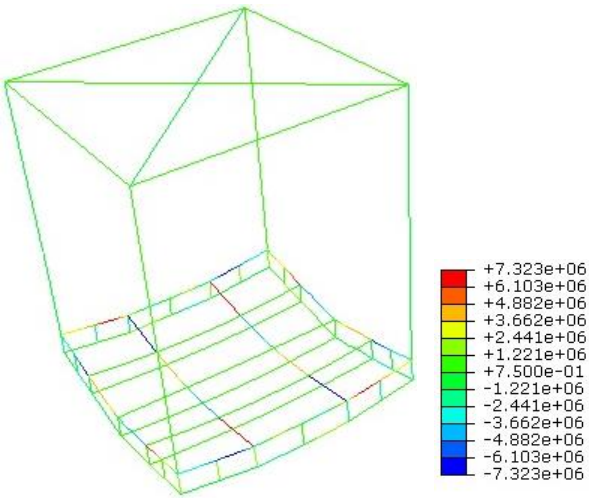

Figure 6. Shear stresses τ_{12} in [Pa].

In addition to the above, a more detailed calculation is performed, involving one of the connection lugs, in order to determine the stress distribution under working load. The results are shown in Figs. 8 and 9 for stresses and displacements, respectively. Once again, the maximal stress value, 40.82 MPa, is much lower than the allowed stress, 213 MPa, in this case.

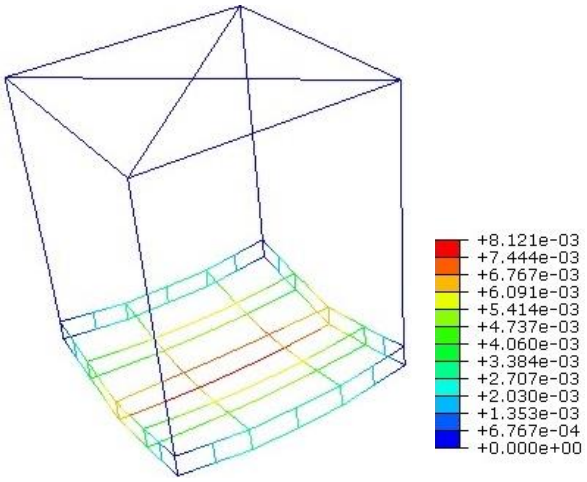

Figure 7. Maximum total displacement.

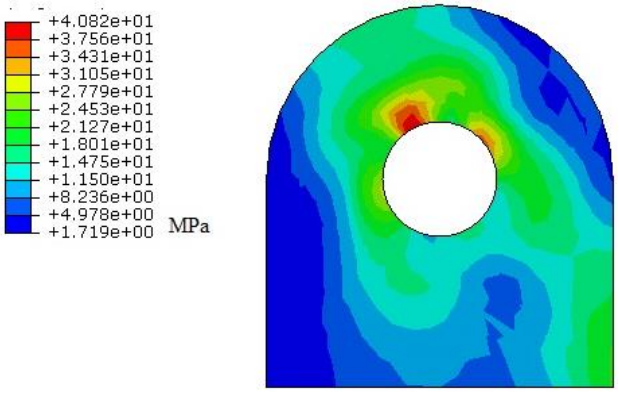

Figure 8. Equivalent stress according to Hencky-Misses in [Pa].

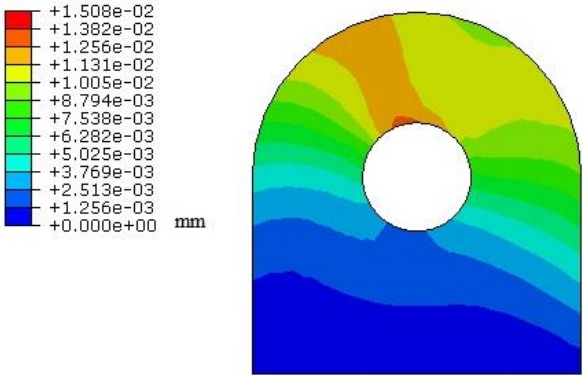

Figure 9. Maximum displacement in mm (f_{max} = 0.01508).

In addition to numerical simulations, fracture mechanics analysis is performed in order to assess how the lug would behave in the presence of a crack, which is assumed to initiate in the location where maximal stress is observed. Since the stresses in this case are relatively low compared to the allowed, a more conservative approach is adopted, and critical crack lengths are based on cases where the stress would be equal to yield stress and tensile strength of the material (235 MPa and ~350 MPa, respectively). Critical crack length in this case corresponds to the value of critical stress intensity factor (K_{Ic}), also known as fracture toughness, /14/, which represents both a fracture mechanics parameter used for linear-elastic calculations and a material property. The formula for determining this value is given below:

$$K_{Ic} = Y\sigma\sqrt{\pi a_c}\,, \tag{1}$$

where: Y is the geometry factor that depends on the position of the crack in a body (for surface cracks that go through the entire thickness, this is usually adopted as 1.12); and a_c is the critical crack length.

Literature sources suggest that this value for low-alloyed structural steels ranges from 5200-6300 MPa√mm /14, 15/, and in this case it is assumed to be 5500. These approximations did not have a significant effect on the final results, as is shown in the following section.

Figure 10. Initial stage of the base assembly.

Figure 11. Final stage of the base structure assembly, including the floor plates.

In the case of yield stress, critical crack length corresponding to fracture toughness of 5500 MPa√mm would be around 140 mm, whereas in the case of tensile strength, it would be around 65 mm. Based on the documentation that contains the lug dimensions, it can be concluded that both of these values significantly exceed the lug's dimensions.

This suggests that the presence of a crack in the critical location, as determined by numerical simulation shown above would not have any noticeable effect on its integrity - the lug would fail due to stresses exceeding its load-bearing capacity before the crack could reach critical value. Hence, somewhat approximated literature values for K_{Ic} that are adopted did not affect the results in any meaningful manner, as they are too high for this case to begin with.

The base structure in the manufacturing stage is shown in Figs. 10 and 11, and the installation of the equipment on the supporting base structure in Fig. 12.

Figure 12. Equipment being installed on the base.

CONCLUSIONS

Presented is the numerical simulation of the behaviour of a supporting base structure used for power equipment used in mining, along with a focus on fracture toughness K_{Ic}. The first part of research is performed with the goal to determine maximal displacements and stresses in the equipment that are below allowed values, and it is confirmed that all values are well within these limits.

The goal of fracture mechanics analysis is to determine how one of the supporting lugs in the base structure behave in the presence of a crack, wherein critical crack length is determined based on known fracture toughness values for the material (steel S235JRG2). Based on the above, it is concluded that critical crack lengths exceed the actual lug dimensions by a considerable amount.

Obtained results suggest that the method presented here is sufficiently accurate and effective at determining the structural integrity of mining equipment by relying on finite element method simulations and relevant fracture mechanics parameters.

ACKNOWLEDGEMENT

This work is supported by the Ministry of Science and Technological Development of Serbia funded projects TR 35011 and TR 35040.

REFERENCES

1. Wang, G. (2013), *New development of longwall mining equipment based on automation and intelligent technology for thin seam coal*, J Coal Sci. Eng. (China) 19: 97-103. doi: 10.1007/s 12404-013-0116-5
2. Guo, W., Xu, F. (2016), *Numerical simulation of overburden and surface movements for Wongawilli strip pillar mining*, Int. J Mining Sci. Technol. 26(1): 71-76. doi: 10.1016/j.ijmst.2015. 11.013
3. Bošnjak, S.M., Zrnić, N.Đ. (2012), *Dynamics, failures, redesigning and environmentally friendly technologies in surface mining systems*, Archiv. Civ. Mech. Eng. 12: 348-359. doi: 10. 1016/j.acme.2012.06.009
4. Javaherdashti, R., Nikraz, H. (2010), *On the role of deterioration of structures in their performance; with a focus on mining industry equipment and structures*, Mater. Corr. 61(10): 885-890. doi: 10.1002/maco.200905515
5. Wang, Y., He, M., Yang, J., et al. (2020), *Case study on pressure-relief mining technology without advance tunneling and coal pillars in longwall mining*, Tunnel. Underg. Space Technol. 97: 103236. doi: 10.1016/j.tust.2019.103236
6. Zhang, Q., Zhang, Y., Guo, S., et al. (2015), *Design and application of solid, dense backfill advanced mining technology with two pre-driving entries*, Int. J Mining Sci. Technol. 25(1): 127-132. doi: 10.1016/j.ijmst.2014.12.008
7. Kollbruner, C.F., Hajdin, N., Dunnwandige Stabe, Band 1, Springer Verlag, 1972.
8. Timoshenko S. Goodier, J.N., Theory of Elasticity, 2nd Ed., McGraw-Hill Book Co., Inc., 1951.
9. Maneski, T., Milošević-Mitić, V., Anđelić, N., Milović, Lj. (2008), *Overhaul and reconstruction of an autoclave*, Struct. Integ. and Life, 8(3): 171-180.
10. Đorđević, B., Sedmak, S., Tanasković, D., et al. (2020), *Failure analysis and numerical simulation of slab carrying clamps*, Frattura ed Integrità Strutturale, 15(55): 336-344. doi: 10.3221/ IGF-ESIS.55.26
11. Jovičić, R., Sedmak, S., Tatić, U., et al. (2015), *Stress state around imperfections in welded joints*, Struct. Integ. and Life, 15(1): 27-29.
12. Grbović, A., Kastratović, G., Sedmak, A., et al. (2019), *Determination of optimum wing spar cross section for maximum fatigue life*, Int. J Fatig. 127: 305-311. doi: 10.1016/j.ijfatigue.2 019.06.019
13. Thiele, Á., Hošek, J. (2015), *Mechanical properties of medieval bloomery iron materials - Comparative tensile and Charpy-tests on bloomery iron samples and S235JRG2*, Period. Polytech. Mech. Eng. 59(1): 35-38. doi: 10.3311/PPme.7760
14. Sedmak, A., Sedmak, S., Milović, Lj., Pressure Equipment Integrity Assessment by Elastic-Plastic Fracture Mechanics Method, Society for Structural Integrity and Life, 2011.
15. Kossakowski, P. (2012), *Simulation of ductile fracture of S235JR steel using computational cells with microstructurally-based length scales*, J Theor. Appl. Mech. 50(2): 589-607.